

Structure and properties of the glandular surface in the digestive zone of the pitcher in the carnivorous plant *Nepenthes ventrata* and its role in insect trapping and retention

Elena Gorb^{1,*}, Victoria Kastner¹, Andrei Peressadko¹, Eduard Arzt¹, Laurence Gaume², Nick Rowe² and Stanislav Gorb¹

¹Evolutionary Biomaterials Group, Max Planck Institute for Metals Research, Heisenbergstr. 3, D-70569 Stuttgart, Germany and ²Botanique et Bioinformatique de l'Architecture des Plantes, UMR CNRS 5120, Boulevard de la Lironde – TA40/PS2, F-34398 Montpellier, Cedex 5, France

*Author for correspondence (e-mail: o.gorb@mf.mpg.de)

Accepted 3 June 2004

Summary

Carnivorous plants of the genus *Nepenthes* grow in nutrient-poor habitats and have evolved specialised trapping organs, known as pitchers. These are composed of different surface zones serving the functions of attraction, capture and digestion of insects, which represent a main source of nitrogen. To investigate the role of the glandular digestive zone in the trapping mechanism of the pitcher, structural, mechanical and physico-chemical studies were applied to *N. ventrata* and combined with insect behavioural experiments. It was found that the glandular surface is microscopically rough since it is regularly structured with multicellular glands situated in epidermal depressions. The presence of downward-directed 'hoods' over the upper part of glands and sloped depressions in the proximal direction of the pitcher causes a marked anisotropy of the surface. The glandular zone surface is composed of relatively stiff material (Young's modulus, 637.19±213.44 kPa). It is not homogeneous, in terms of adhesive properties, and contains numerous areas without adhesion as well as adhesive areas differing greatly in tenacity values (range, 1.39–28.24 kPa). The surface is readily wettable with water (contact angle, 31.9–36.0°C) and has a high surface free energy (56.84–61.93 mN m⁻¹) with a relatively high polar component (33.09–52.70 mN m⁻¹). To examine the effect of the glandular secretion on attachment systems of insects having hairy and smooth adhesive pads, forces generated on different surfaces by *Calliphora vicina* flies and *Pyrhcoris apterus* bugs, respectively, were

measured. Flies attached equally well to both fresh and air-dried glandular surfaces whereas bugs generated a significantly lower force on the fresh glandular surface compared with the air-dried one. It is assumed that the contribution of the glandular surface to insect retention, due to its effect on insect attachment, differs depending on insect weight and the type of insect attachment system. Surface anisotropy does not facilitate effective claw interlocking so that insects possessing only claws are probably not able to cling to the glandular surface. However, stiffness of the pitcher wall material in the digestive zone can provide claw clinging *via* punching of the pitcher wall by claws. Small insects lacking pads may use adhesive areas on the plant surface to attach themselves, but such solitary points with very strong adhesion possibly impede their overall locomotion and chance of escape. Pad-bearing insects are presumably able to attach to smooth parts of the glandular surface located between glands. High free surface energy of the plant substrate may promote adhesion. Gland secretion may decrease attachment ability in insects with smooth adhesive pads but not influence attachment of insects with hairy attachment systems.

Key words: trapping function, insect, insect attachment, smooth/hairy attachment, fly, *Calliphora vicina*, bug, *Pyrhcoris apterus*, profile, elasticity, Young's modulus, adhesion, tenacity, surface free energy, claw interlocking, adhesive pad, friction force.

Introduction

Carnivorous plants possess modified organs as trapping devices that capture insects and other small animals and use them as a main nitrogen source. Among them are active traps that involve active plant movement (such as *Dionaea muscipula*, *Drosera* spp. and *Utricularia* spp.) and passive traps that involve no movement (Lloyd, 1942). In the latter,

three types of highly specialised structures have evolved: (1) adhesive traps of *Drosophyllum* spp., *Byblis* spp. and *Roridula* spp., (2) lobster pot traps of *Sarracenia psittacina* and *Genlisea* spp. and (3) pitfall traps of plants from the families Nepenthaceae, Sarraceniaceae, Cephalotaceae and Bromeliaceae (Slack, 2000). In pitcher plants, despite

extremely different morphologies, the traps have been optimised, by natural selection, to serve different functions, such as attracting and trapping animals, preventing escape of prey, digestion and nutrient absorption (Juniper et al., 1989). The pitcher's structure is not uniform but consists of different structural and functional zones (Lloyd, 1942) having specialised macro- and micromorphological features and serving a variety of functions.

In most *Nepenthes* species, the pitcher is composed of a lid, a peristome (ribbed upper rim of the pitcher), a waxy zone and a digestive zone with a pool of digestive fluid (Adams and Smith, 1977; Owen and Lennon, 1999). These zones differ greatly in their geometry, structure, surface architecture and functions. The lid and the peristome of pitchers are supposed to be involved in animal attracting and trapping (Jebb and Cheek, 1997; Owen and Lennon, 1999; Gaume et al., 2002), and the waxy zone has been widely studied for its implications in trapping and preventing the escape of prey (Lloyd, 1942; Juniper and Burras, 1962; Juniper et al., 1989; Gaume et al., 2002, 2004). By contrast, the digestive zone is believed to contribute solely to prey utilisation. For this reason, the digestive zone has been studied mostly for its chemical function in digestion, absorption and transport of the insect-derived nitrogen compounds (Juniper et al., 1989; Schulze et al., 1999; Owen et al., 1999; An et al., 2001). However, this zone may also influence the trapping efficiency of the pitcher, since animals are usually captured and drawn into the digestive fluid (Juniper et al., 1989; Adams and Smith, 1977; Owen and Lennon, 1999). Recent experiments with flies (*Drosophila melanogaster*) and ants (*Iridomyrmex humilis*) on epidermal surfaces of the *Nepenthes alata* pitchers showed that the glandular secretion probably acts mechanically, like a glue, and impedes insect locomotion (Gaume et al., 2002).

The principal aim of the present study is to investigate whether the glandular surface of the digestive zone in pitcher plants is also involved in the trapping and retention mechanism. This surface may constitute an area for retaining insects. We hypothesise that (1) the roughness of the glandular surface does not accommodate claw interlocking; (2) stiffness of digestive zone material precludes both claw and pad attachment; (3) adhesive properties of the surface prevent insect attachment and locomotion and (4) gland secretion lessens insect adhesive pad attachment. To test this, structural and biomechanical studies of the glandular surface of *Nepenthes ventrata* were combined with insect behavioural experiments. Laboratory experiments were carried out on fresh and air-dried glandular surfaces with flies (*Calliphora vicina*) and bugs (*Pyrrhocoris apterus*). The two species have adhesive pads of two different types: hairy and smooth, respectively. The following questions were asked: (1) which morphological features of the glandular surface may contribute to trapping insects, (2) do mechanical properties of the digestive zone, such as plant material elasticity, adhesive properties and surface free energy of the glandular surface, promote insect retention and (3) how does the presence of gland secretion influence insect attachment?

Materials and methods

Plant and insect species

The pitcher plant *Nepenthes ventrata* Hort. ex Fleming [= (*N. ventricosa* Blanco × *N. alata* Blanco) Phil.] (Nepenthaceae Dumort.) is a natural hybrid found in the northern forests of the Philippines (Clarke, 2001). Plants were obtained from a nursery and grown in small greenhouses under controlled shaded conditions at 20–24°C and 70–90% humidity. Plants were watered daily with distilled water.

The two insect species used in friction tests were selected for similarity in size (values are means ± s.d.; fly body length=9.33±0.44 mm, *n*=15; bug body length=9.30±0.60 mm, *n*=15) and weight (fly mass=44.58±10.67 mg, *n*=15; bug mass=42.67±8.59 mg, *n*=15). They bear adhesive pads belonging to two alternative types of locomotory attachment devices in insects (Gorb and Beutel, 2001; Beutel and Gorb, 2001; Gorb, 2001). The fly *Calliphora vicina* Robineau-Desvoidy (Diptera, Brachycera, Calliphoridae) possesses hairy pulvilli, whereas the bug *Pyrrhocoris apterus* L. (Hemiptera, Heteroptera, Pyrrhocoridae) has smooth ones. Both types of attachment pads have been reported to produce secretory fluid, which is delivered onto the contact area during contact formation with the substrate (Hasenfuss, 1977, 1978; Bauchhenss, 1979; Walker et al., 1985; Gorb, 1998, 2001). Representatives of both insect orders were reported to be captured by the traps of *Nepenthes* plants (Juniper et al., 1989; Kato et al., 1993; Moran, 1996; Moran et al., 1999). Flies were taken from a laboratory colony at the University of Würzburg (Germany) and kept in a small terrarium at 20–24°C, 65–70% humidity. Insects were fed with crystalline sugar and tap water. Bugs were collected in a lime-tree garden in Tübingen (Germany) and used on the same day.

Structural studies

The general organisation of the glandular surface in the digestive zone and gland arrangement were studied on a fresh, untreated pitcher surface with a binocular microscope (Leica MZ 12.5) with a built-in video chip (Leica IC A) and a scanning electron microscope (SEM). For SEM, small pieces (~1 cm²) of the pitcher wall were cut out with a razor blade from the upper and middle parts of the digestive zone, mounted on holders and examined, without sputter-coating, in a Hitachi S-800 scanning electron microscope at 5 kV. Gland dimensions as well as the density of the glands per mm² were quantified from digital images using SigmaScan software (SPSS Inc., Chicago, IL, USA).

The surface profile was studied on fresh, untreated samples (~1 cm²) cut out, using a razor blade, of the upper and middle parts of the digestive zone and glued with double-sided tape to a glass slide. The samples were examined in a scanning white-light interferometer (Zygo NewView 5000; Zygo Corporation, Middlefield, CT, USA) using objectives 20 and 50 at magnifications of 20×0.4, 20×1.3, 20×2.0, 50×0.4, 50×1.3 and 50×2.0. The device included optics for imaging an object surface and a reference surface together onto a solid-state imaging array, resulting in an interference intensity pattern that

was read electronically into a computer. A series of interferograms were generated as the objective was scanned perpendicular to the illuminated surface. They were then individually processed, and finally a complete 3-D image, constructed from the height data and corresponding image plane coordinates, was created. From 3-D images, profilograms of sections with and without glands as well as height parameters were obtained.

For anatomical studies of digestive glands, tissue specimens (~1 cm²) were cut out, using a razor blade, of the middle part of the digestive zone, fixed overnight in a 5% sucrose solution in a desiccator under vacuum, infiltrated in 15% and 30% sucrose solutions, embedded in Tissue-Tek® (O.C.T. Compound Sakura Finetek USA, Inc., Elkhart, IL, USA), frozen and sectioned in longitudinal and transverse planes perpendicular to the surface using a cryotome Leica CM 3050. Sections (7, 10 and 14 µm thick) were collected on pre-coated glass slides, both unstained and stained for 0.5 min with a warm (60°C) ethanol solution of Sudan Black, rinsed for 1 min in 50% ethanol, mounted in mounting medium (Depex; Serva, Heidelberg, Germany) and analysed in a light microscope (Zeiss Axioplan) under bright-field conditions and under phase contrast. In addition, unstained sections and fresh non-sectioned tissue specimens were mounted on a glass slide and checked for autofluorescence using fluorescence microscopy with an HBO 100 W/2 UV filter pack (Carl Zeiss, Germany) in one of three bands of wavelength: green (excitation 512–546 nm; emission 600–640 nm), red (excitation 710–775 nm; emission 810–890 nm) and UV bands (excitation 340–380 nm; emission 425 nm). Digital images were obtained using a Zeiss AxioCam MRc video camera mounted on the light microscope.

To obtain detailed information about the attachment devices in the insect species used in the experiments, tarsi were cut from legs, fixed in 70% ethanol, dehydrated in an increasing series of ethanol, critical-point-dried, mounted on holders, sputter-coated with gold–palladium (10 nm) and examined in the SEM at 20 kV. After friction experiments (see below), insects were killed by freezing individually at –20°C in small plastic jars. The insects were returned to room temperature, air-dried, mounted on holders, sputter-coated with gold–palladium and studied in the SEM.

Estimation of material properties

The material properties of the digestive zone were measured with a micro-force measurement device (Basalt-BT01; Tetra GmbH, Ilmenau, Germany; Gorb et al., 2000; Jiao et al., 2000). A small piece (~1 cm²) of the pitcher wall, cut out of the middle part of the glandular digestive zone with a razor blade and glued with double-sided tape to a platform, was used as a lower sample (Fig. 1). A small sapphire sphere (0.75 mm in radius), connected to a glass spring with a spring constant of 290 N m⁻¹, was an upper sample. The sphere was brought into contact with the plant sample to set a normal force of 300–1800 µN, which corresponded to the weight of middle-sized and large syrphid flies (Gorb et al., 2001), and

then retracted from the surface. After each measurement, the sapphire sphere was cleaned with acetone. The recorded force–distance curves were used to calculate the elasticity of the plant sample (loading process) and to estimate the adhesion force (retracting process) (Fig. 2). Experiments were carried out at room temperature (20–25°C) at a relative humidity of 58–76%. Three pitchers from three different plants were tested. Elasticity was estimated from five randomly chosen points (1–2 tests per point; in total, 7 tests); adhesion was measured at 23 points (1–10 tests per point; in total, 85 tests).

The plant surface deformed when the sapphire sphere pressed against the sample. The indentation of the plant material was obtained by comparing the spring deflections induced by the plant sample and a hard sample (a glass plate). By subtracting the displacement of the plant sample from that of the hard sample at the same spring deflection under the same applied force, the indentation of the plant material was calculated (Gorb et al., 2000; Jiao et al., 2000).

To estimate the elasticity of the digestive zone tissue, the Hertz theory (Hertz, 1881), describing the deformation of two smooth elastic bodies in contact under applied force, was used. The relationship between the indentation (δ) and the applied force (F_n) is given by:

$$\delta = F_n/Ka, \quad (1)$$

where K is the reduced elasticity modulus of materials and a is a radius of the circular contact area. K is related to the Young's modulus as:

$$K = \frac{4}{3} \left(\frac{1 - \nu^2}{E} + \frac{1 - \nu_b^2}{E_b} \right)^{-1}, \quad (2)$$

where E and ν are the Young's modulus and Poisson ratio of the plant sample, respectively, and E_b and ν_b are the same parameters for the sapphire sphere. Since the material of the sapphire sphere is much stiffer than that of the plant sample tested ($E_b \gg E$):

$$K \cong \frac{4}{3} \frac{E}{1 - \nu^2}. \quad (3)$$

Contact radius, a , depends on the indentation depth and the sapphire sphere radius (R) as:

$$a^2 = R\delta. \quad (4)$$

Equations 1, 3 and 4 imply that the indentation can be expressed with applied force as:

$$\delta = \frac{F_n^{\frac{2}{3}}}{K^{\frac{2}{3}}R^{\frac{1}{3}}} = \left(\frac{3}{4} \frac{1 - \nu^2}{E} \right)^{\frac{2}{3}} \frac{F_n^{\frac{2}{3}}}{R^{\frac{1}{3}}}. \quad (5)$$

From equation 5, the Young's modulus of the plant material was calculated.

To compare data on adhesion at different points of the glandular surface, obtained with different normal forces

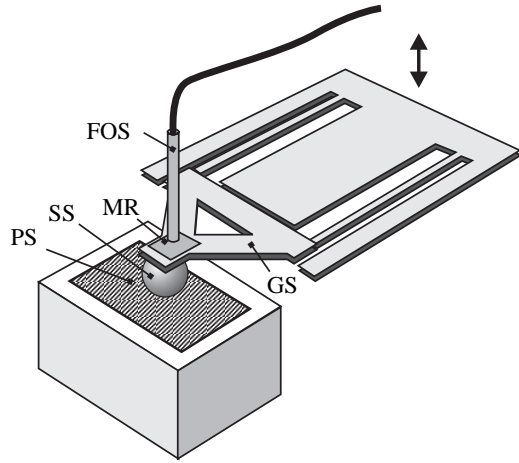


Fig. 1. Experimental set-up for estimation of material properties by microindentation. SS, sapphire sphere; FOS, fibre optical sensor; GS, glass spring; MR, mirror; PS, plant sample.

applied, tenacity T (the adhesive force, F_a , per unit of contact area) was used:

$$T = F_a/A, \quad (6)$$

where A is contact area. From the Hertz theory, for two elastic bodies in contact:

$$A = \pi a^2. \quad (7)$$

By substituting equations 4, 5 and 7 into equation 6, we obtain:

$$T = F_a/\pi a^2 = F_a/\pi R\delta = \frac{F_a}{\pi} \left(\frac{K}{RF_n} \right)^{\frac{2}{3}}. \quad (8)$$

However, in the retracting process, because of the adhesion found, the deformation from both applied force and surface energy should be considered (Johnson et al., 1971). In the present study, we did not take adhesive forces into account and considered the deformation to be caused by the applied force alone.

Contact angle measurements and evaluation of surface free energy

Estimates of surface free energy and its components on the glandular surface of the digestive zone were carried out with a high-speed optical contact angle measuring device (OCAH 200; DataPhysics Instruments GmbH, Filderstadt, Germany). The device was equipped with a high-speed CCD video system, four manual and/or electronic (motor-driven and software-controlled) dosing units with a manual or electronic multiple-dosing system, micro-controller module for control of the electronic syringe units and motor-driven sample stages. The software offered static contact angle measurements according to the sessile drop method, estimation of the surface free energy of solids and their components according to standard evaluation methods, and provided statistics and measurement error analysis (Maier, 2002).

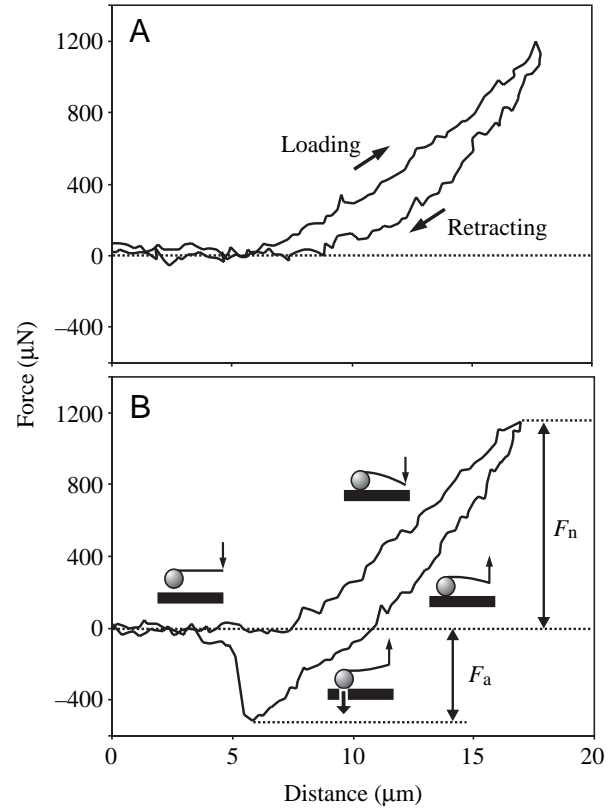


Fig. 2. Typical force–distance curves used for evaluation of elasticity and adhesive properties of the surface. (A) Without adhesion. (B) With adhesion. F_a , adhesion force; F_n , maximal applied force; Loading, part of the curve corresponding to the loading process; Retracting, part of the curve corresponding to the retracting process.

A series of well-characterised liquids (water, density=1.000 kg m⁻³; diiodomethane, density=3.325 kg m⁻³; ethylene glycol, density=1.113 kg m⁻³) were used to calculate the surface free energy of the glandular surface. Using the sessile drop method (drop volume 2 µl) with circle or ellipse fitting, static contact angles of liquids to the surface were evaluated on fresh, untreated glandular tissue. Samples (3–6 cm²) were cut out using a razor blade from the upper and middle parts of the digestive zone and then attached with double-sided tape to a glass slide. The surface free energy and dispersion and polar contributions of the surface energy were calculated according to two universal methods: Owens–Wendt–Kaelble (Owens and Wendt, 1969) and Wu (Wu et al., 1995). The surface free energy of three pitchers belonging to three plants was calculated. For each pitcher, 3–5 measurements of the contact angle of each liquid to the surface were conducted with a total of 39 measurements.

Friction experiments with insects

Friction experiments with two insect species were designed to study the influence of glandular surface on the functional efficiency of the insect attachment systems composed of claws and adhesive pads of two alternative designs: smooth and hairy. Two questions were asked: (1) does the glandular

surface covered with gland secretion lessen insect attachment and (2) how does the glandular surface affect attachment systems with different pad designs?

Force measurements were carried out with a load cell force transducer (10 g capacity; Biopac Systems Ltd, Santa Barbara, CA, USA) (Gorb and Popov, 2002). Experimental insects were made incapable of flying, prior to experiments, by either gluing the forewings together (bugs) with a small droplet of molten wax or cutting off the wings (flies). The insect was attached to the force sensor by means of a hair (10–15 cm long) glued to the dorsal surface of the insect thorax with a drop of molten wax (Fig. 3A). Plant surface samples (6–15 cm²) were cut out of the digestive zone using a razor blade and then, either fresh or air-dried, connected with double-sided tape to a horizontal glass plate so that insects had to move from the bottom to the upper part of the zone, simulating the situation of escaping from the bottom of the pitcher. Three types of substrates were used: (1) fresh glandular surface, (2) glandular surface that had been air-dried for 3–5 days at 20–24°C, 60–75% humidity and (3) a glass plate as a control. The force generated by the insect walking horizontally on the test substrates was measured. Force–time curves were used to estimate the maximal friction force produced by insects (Fig. 3B). Experiments were carried out at 23°C and 76% humidity. For each substrate type, experiments with five individual flies and five individual bugs (4–5 repetitions per insect) were conducted. Five pitchers from five different plants were tested. In all, 30 insects were used and 149 individual tests were carried out.

Results

Glandular surface morphology

General morphology of the glandular surface in the digestive zone

The digestive zone constitutes approximately half of the pitcher height, and tested pitchers contained digestive fluid for a quarter to a third of the vertical extent of the glandular surface. The glandular surface bears small oval depressions, each having a gland at its base (Fig. 4A). The depth of the depressions decreases from the top to the bottom of the digestive zone. Each gland is partly covered by a small ‘hood’ overhanging the upper margin of each depression (Fig. 4B,C). The dimensions and prominence of the hoods decrease towards the proximal direction (towards the base) of the pitcher so that the hoods become almost unnoticeable, and the glands at the bottom of the pitcher are exposed.

Both the shape and size of the glands vary depending on the level of the digestive zone. Glands of the upper part are smaller (area=12563.31±5420.47 μm², mean ± s.d., *n*=30 samples, *N*=3 pitchers), almost round or slightly elongated in the longitudinal direction. In the centre of the zone, glands are larger (area=49101.90±10843.28 μm², *n*=30, *N*=3), round or slightly elongated in the transverse direction. Glands situated at the bottom of the pitcher are much larger (area=92242.52±14139.50 μm², *n*=15, *N*=3), round or noticeably elongated in the transverse direction. Density of the

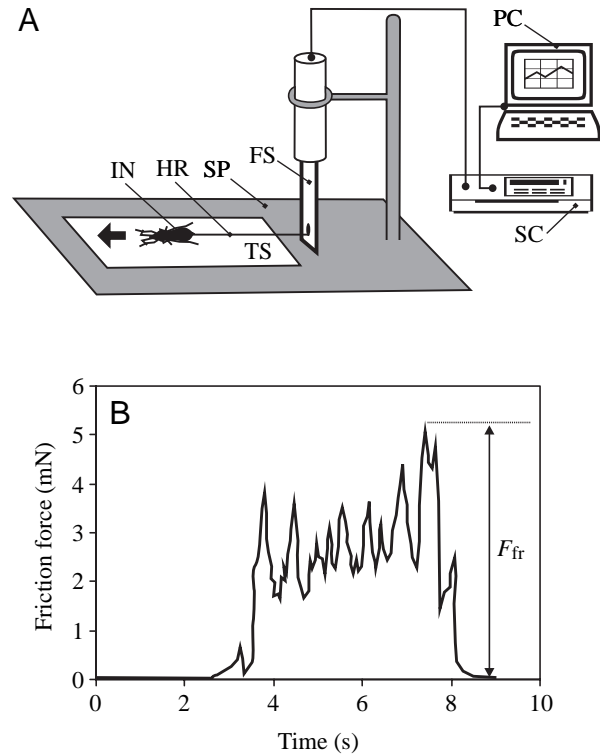


Fig. 3. Experimental set-up for friction force measurements (A) and a typical force–time curve (B) used for estimation of maximal friction force (F_{fr}) generated by insects. FS, force sensor; HR, hair; IN, insect; PC, computer; SC, sensor control; SP, support; TS, tested surface.

glands is considerably higher in the distal part of the digestive zone (8.87 glands mm⁻², *n*=15, *N*=3) than at the bottom of the pitcher (3.72 glands mm⁻², *n*=15, *N*=3).

The surface of the gland is not even but corrugated and bears small scale-like irregularities (Fig. 4D,E). On the surface of some glands, beam-shaped crystals are found (Fig. 4E).

Surface profile

The surface of the glandular zone is regularly covered with glands. The surface between glands is relatively smooth and shows small height differences at low magnification in the white-light profilometer (objective 50, magnification 50×0.4). At a higher magnification (objective 50, magnification 50×2.0), the surface appears to be uniformly structured with almost similar irregularities (height, 0.1–0.4 μm; length, 3.0–5.0 μm) (Fig. 5A,B).

Glands show different profiles in the upper (Fig. 5C,D) and middle (Fig. 5E,F) parts of the digestive zone. In both cases, they are located in deep (22–28 μm) depressions with downward-projecting hoods distally and a slope slanting in the proximal direction of the pitcher. However, the height of the actual gland and hood can vary over the digestive zone: at the top, glands are lower (11–14 μm) and hoods higher (25–28 μm) than those of the middle part (both glands and hoods: 14–16 μm). In upper glands, both the upper slope surface and at least part of the central region are covered by

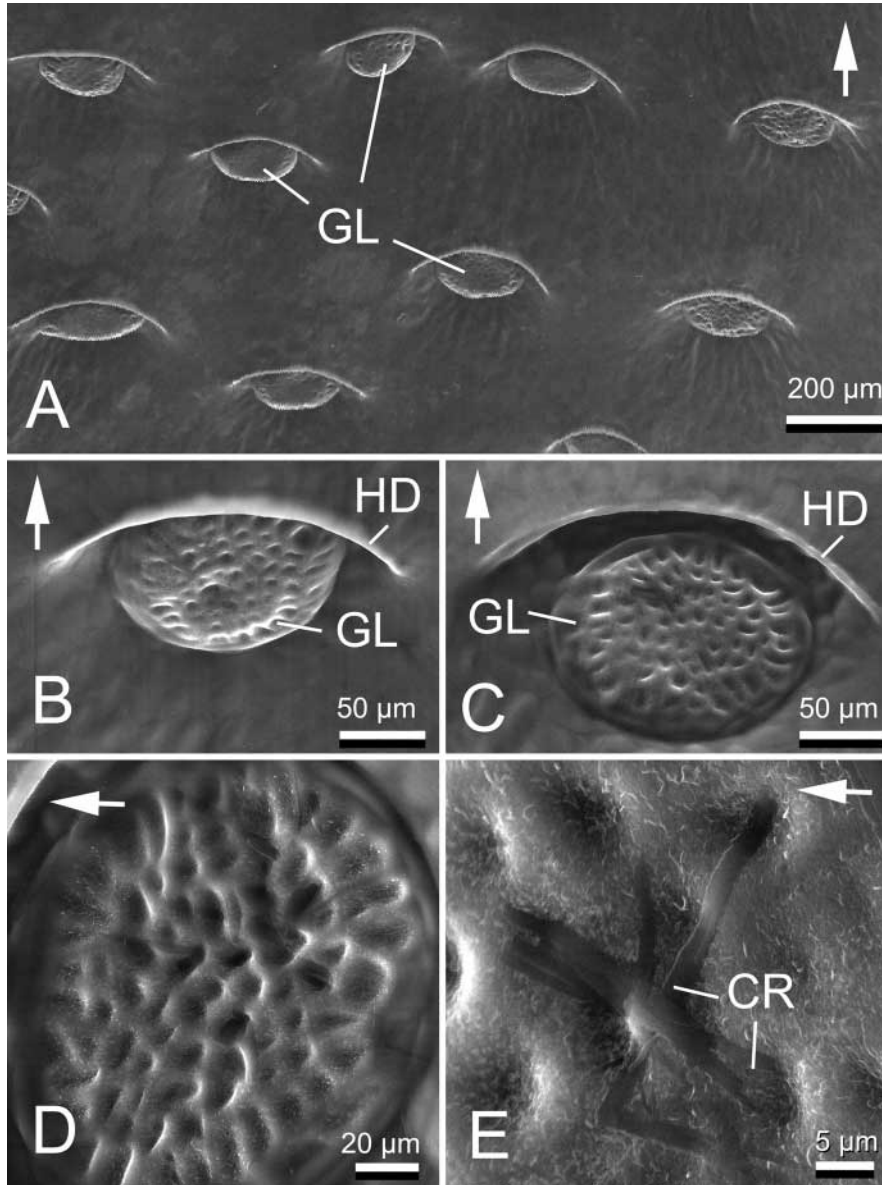


Fig. 4. SEM micrographs of the glandular surface. (A) General view of the surface. (B) Gland of the upper part of the digestive zone. (C) Gland of the middle part of the digestive zone. (D) Surface of the gland. (E) Crystals on the gland surface. Arrows show the direction to the peristome. CR, crystal; GL, gland; HD, hood.

(outer epidermis, length= $15.71 \pm 3.22 \mu\text{m}$, width= $25.90 \pm 10.55 \mu\text{m}$, $n=23$; inner epidermis, length= $14.81 \pm 5.02 \mu\text{m}$, width= $28.16 \pm 10.18 \mu\text{m}$, $n=30$). The optical properties of the outer wall of the inner epidermis differ from those of the internal wall and the walls of mesophyll cells. The outer wall shows weak autofluorescence in UV light (Fig. 7A,B). Mesophyll cells are thin-walled, relatively large (length= $33.35 \pm 11.25 \mu\text{m}$, width= $42.63 \pm 12.79 \mu\text{m}$, $n=37$) and irregularly shaped. Vascular bundles are present in the mesophyll tissue.

In the inner surface of the pitcher wall, glands are distributed equally, and each is situated at the bottom of a small epidermal depression and either does not extend beyond it or protrudes from the epidermal surface to a maximum of no more than half the thickness of the gland (Fig. 6B,C). Sections indicate that the hood, called the epidermal ridge, is comprised of a modified epidermal cell extending over at least part of the depression, as described above (Fig. 6B). The hood may also appear as paired structures surrounding the gland on each side (transverse sections across the upper part of the gland; Fig. 6C). The entire hood shows weak autofluorescence

the hoods, whereas in glands situated at lower levels of the digestive zone only the upper slope surface is hooded.

Generally, downward-pointing hoods and the slanting slopes of depressions result in the anisotropy of the glandular surface profile. This anisotropy is less developed in the middle part of the digestive zone and significantly reduced at the bottom of the pitcher.

Anatomy of the digestive zone

In both longitudinal and transverse sections of the digestive zone, the pitcher wall appears as a layered structure (thickness= $212.28 \pm 31.50 \mu\text{m}$, $n=12$, $N=4$) with an outer epidermis facing the environment, a layer of inner epidermis facing the trap cavity, and a multilayered spongy mesophyll in between (Fig. 6A). The epidermal cells are covered with cuticle, are thick-walled (especially outer walls) and vary greatly in shape (from almost round to oval, laterally elongated) and size

in UV light in whole-mount surface preparations (Fig. 7C).

The gland is a multicellular structure consisting of three cell layers. Although an epidermis is absent from the gland, a thin (up to $1 \mu\text{m}$ thick) cuticle covers its surface (Fig. 6D). The outermost cell layer, known as a glandular head (terminology from Juniper et al., 1989), consists of columnar cells (Fig. 6D–F) that do not vary much in shape but do vary in size (longitudinal sections, length= $22.59 \pm 5.11 \mu\text{m}$, width= $14.42 \pm 2.65 \mu\text{m}$, $n=52$; transverse sections, length= $21.82 \pm 4.30 \mu\text{m}$, width= $12.51 \pm 1.15 \mu\text{m}$, $n=39$). The cells bear thicker lateral walls (longitudinal sections, thickness= $2.27 \pm 0.44 \mu\text{m}$, $n=19$; transverse sections, thickness= $2.55 \pm 0.97 \mu\text{m}$, $n=7$) and an extremely thick external wall (longitudinal sections, thickness= $3.47 \pm 0.53 \mu\text{m}$, $n=18$; transverse sections, thickness= $4.08 \pm 0.73 \mu\text{m}$, $n=11$) having different optical properties than the internal walls (Fig. 6D) and walls in other gland cells and mesophyll cells. The external wall differs in its material structure at the inner and outer margins

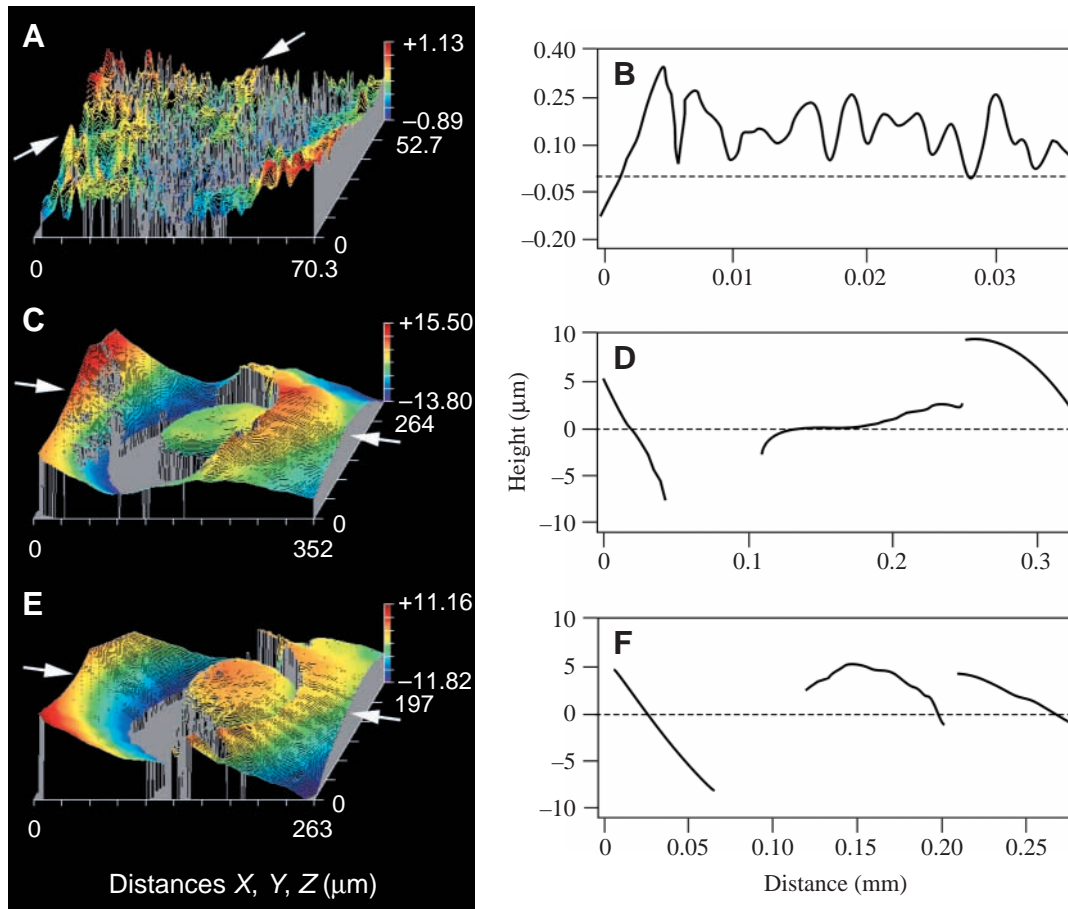


Fig. 5. 3-D images (A,C,E) and profilograms (B,D,F) of different parts of the glandular surface. (A,B) Part between glands (objective 50, magnification 50×0.4). (C,D) Gland in the upper part of the digestive zone (objective 20, magnification 20×1.3). (E,F) Gland in the middle part of the digestive zone (objective 20, magnification 20×2.0). Arrows in A,C,E show the axes for profiles in B,D,F, respectively.

(Fig. 6D). Inner margins are half as thick (longitudinal sections, thickness= $1.22\pm 0.29\ \mu\text{m}$, $n=18$; transverse sections, thickness= $1.26\pm 0.33\ \mu\text{m}$, $n=11$) as outer ones (longitudinal sections, thickness= $2.33\pm 0.44\ \mu\text{m}$, $n=19$; transverse sections, thickness= $2.75\pm 0.81\ \mu\text{m}$, $n=11$). In these cells, as well as in adjoining epidermal cells and in the ridge, the outer margin of the external wall weakly reflects UV light (Fig. 7A,B). Only a few cells of the first layer are found to have cytoplasm. Most cells contain secretion inclusions that may fill up to three-quarters of the cell volume (Fig. 6F).

The cells of the second layer usually vary more in shape (from almost columnar, radially elongated to round or even oval, laterally elongated) and size (longitudinal sections, length= $14.91\pm 3.60\ \mu\text{m}$, $n=35$, width= $19.43\pm 4.70\ \mu\text{m}$, $n=33$; transverse sections, length= $15.64\pm 4.17\ \mu\text{m}$, width= $19.30\pm 3.91\ \mu\text{m}$, $n=30$) than those of the first layer (Fig. 6E–G). These cells have relatively thin walls and have cytoplasm.

The third layer could be clearly observed, mainly in longitudinal sections. It appears as a chain of elements and is composed of large (longitudinal sections, length= $12.00\pm 3.19\ \mu\text{m}$, width= $29.93\pm 7.39\ \mu\text{m}$, $n=11$; transverse sections, length= $10.41\pm 2.77\ \mu\text{m}$, width= $27.20\pm 5.85\ \mu\text{m}$,

$n=15$), in most cases laterally elongated, cells (Fig. 6E,G). As in the cells of the previous layer, these cells have thin walls and cytoplasm. In a very few sections, not a layer but just several separate cells are found beneath the third layer.

A glandular head and cells of the second and third layers comprise the so-called glandular component of the gland. The gland is separated from a sunken epidermal layer and other underlying tissue by a band of laterally elongated and radially flattened cells (longitudinal sections, length= $4.96\pm 1.71\ \mu\text{m}$, width= $29.50\pm 7.09\ \mu\text{m}$, $n=11$; transverse sections, length= $4.35\pm 0.86\ \mu\text{m}$, width= $21.27\pm 3.10\ \mu\text{m}$, $n=12$) with thickened walls (longitudinal sections, thickness= $1.44\pm 0.43\ \mu\text{m}$, $n=15$; transverse sections, thickness= $0.90\pm 0.07\ \mu\text{m}$, $n=4$) (Figs 6G, 7A). In these cells, lateral and partly external and internal walls, as well as lateral walls in cells of the adjoining third gland layer and sunken epidermis, strongly reflect UV light (Fig. 7B). This indicates large deposits of cutin or suberin and is characteristic for an endodermoid component of the gland (Juniper et al., 1989; Owen and Lennon, 1999; Schulze et al., 1999). On whole-mount surface preparations, these walls appear as two nets that differ in mesh dimension (Fig. 7C).

Tracheid elements of vascular bundles are seen close to

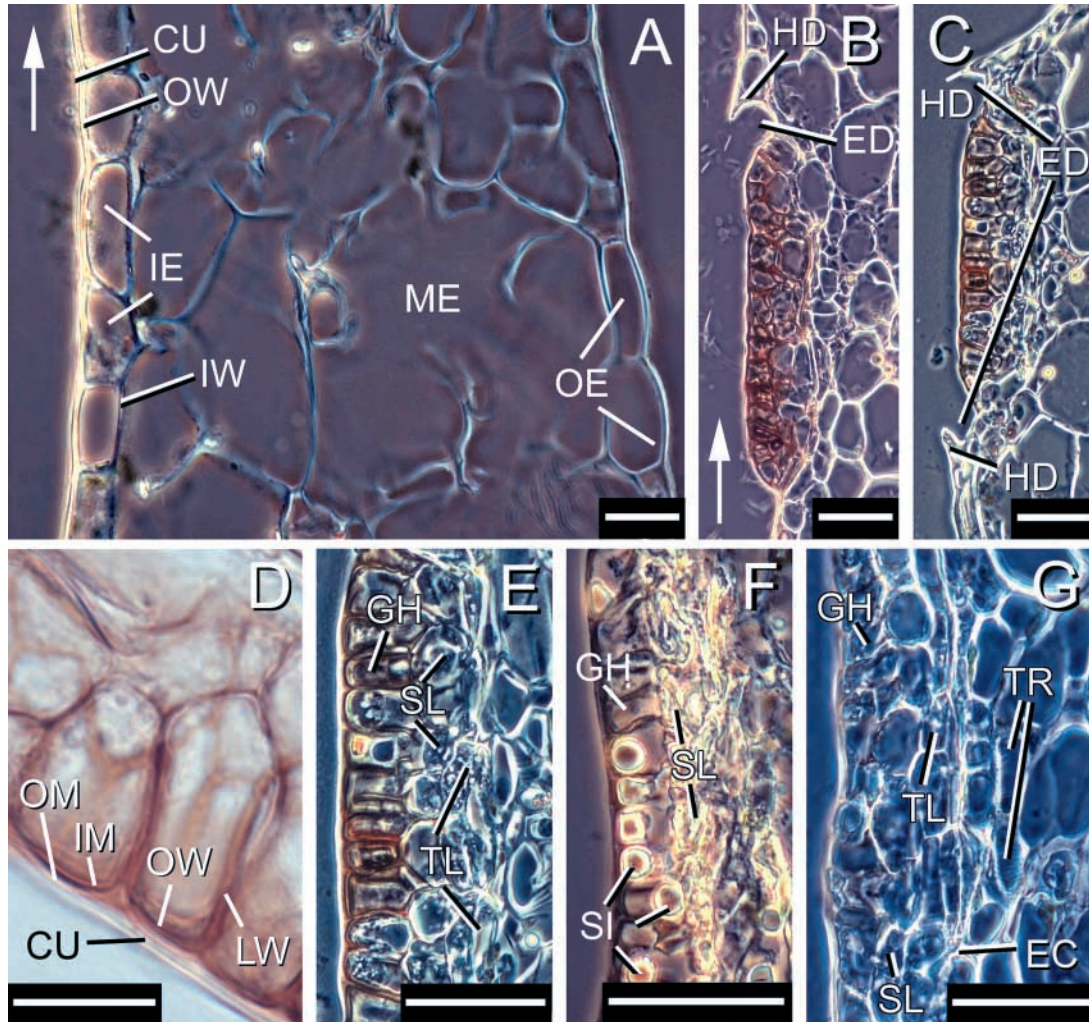


Fig. 6. Anatomy of the digestive zone (light microscopy). (A) Transverse section of the pitcher wall. (B) Longitudinal and (C) transverse sections of the gland, general view. (D) Longitudinal section of the glandular head. (E–G) Transverse sections of the gland. Arrows show the direction to the peristome. CU, cuticle; EC, endodermoid component; ED, epidermal depression; GH, glandular head; HD, hood; IE, inner epidermis; IM, inner margin of the cell wall; IW, internal cell wall; LW, lateral cell wall; ME, mesophyll; OE, outer epidermis; OM, outer margin of the cell wall; OW, outer cell wall; SI, secretion inclusion; SL, second layer of cells; TL, third layer of cells; TR, tracheid element. Scale bar: A,D, 20 μm ; B,C,E–G, 50 μm .

digestive glands (Fig. 6G). Usually they are located one or two layers beneath the base of the gland.

Properties of the glandular surface

Elasticity of the material

The force–time curves indicated that the plant material has visco-elastic properties (Fig. 8A). During the loading process, a gradual deformation of the sample was observed. The deformation fitted well with the Hertz model (nonlinear regression according to equation 5, $P < 0.001$, one-way ANOVA) in the entire range (up to 1800 μN) of the applied force (Fig. 8B). The indentation at the applied forces of 450–1800 μN was 8–16 μm . Since the Poisson ratio known for plant materials ranges from 0.2 to 0.7 (Mohsenin, 1986; Niklas, 1992), we used an average ratio for calculations. By applying the Hertz theory for load forces up to 1800 μN and the Poisson

ratio of 0.5, we obtained the Young's modulus of 637.19 ± 213.44 kPa ($n=7$ points, $N=3$ pitchers).

Adhesive properties

Measurements of the adhesion revealed that the glandular surface was not homogeneous: points with adhesion ($n=14$) and without adhesion ($n=9$) were found. At points with adhesion, the adhesion force varied from 24.74 to 647.32 μN . This variation depended significantly, in decreasing order of importance, on the plant, the applied force and the point of application (Table 1). On the whole, the adhesion increased linearly with the applied force (F_n , significant), but the slope of the relation varied according to the point studied [$F_n \times$ point (plant), significant], while it did not vary significantly according to the plant ($F_n \times$ plant, not significant) (Fig. 9A). Measured at the same point, the adhesion force usually

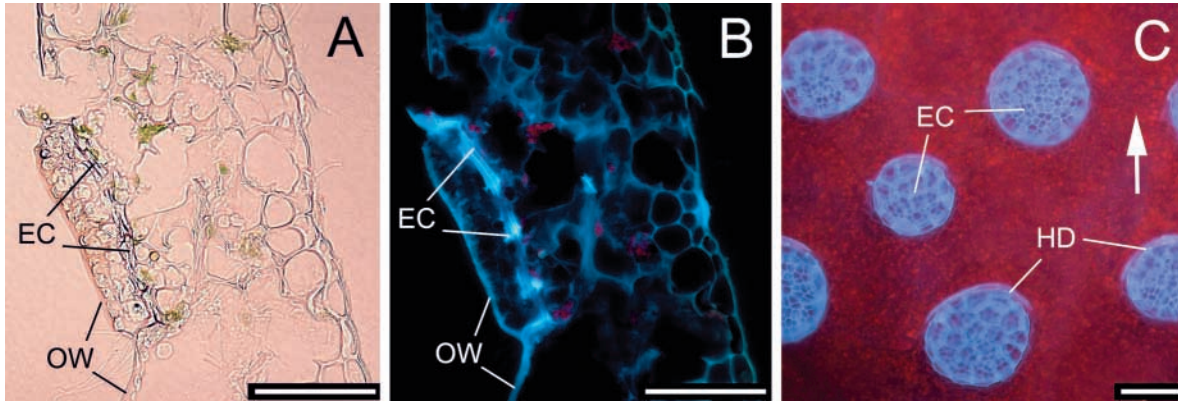


Fig. 7. Anatomy of the digestive zone (fluorescence microscopy). (A,B) Transverse section of the gland in a light (A) and fluorescence microscope (B). (C) Whole-mounted surface preparation in a fluorescence microscope. Arrow shows the direction to the peristome. EC, endodermoid component; HD, hood; OW, outer cell wall. Scale bar: 100 μm .

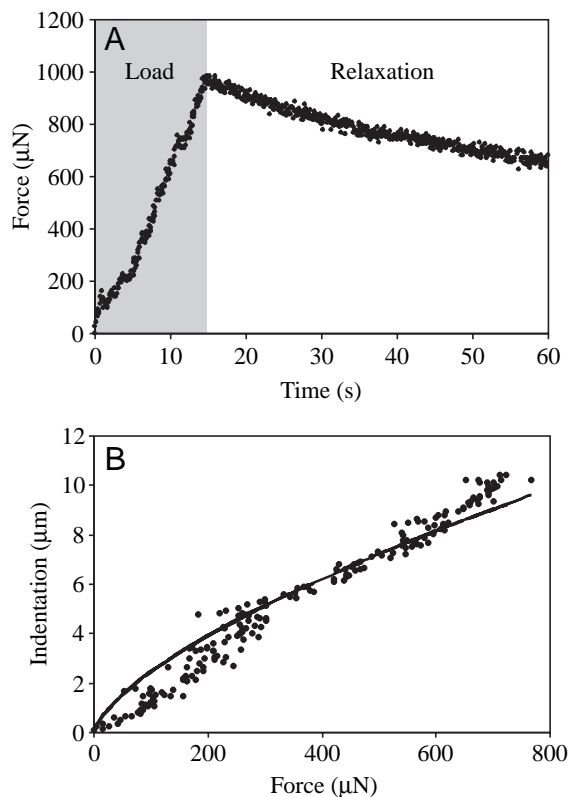


Fig. 8. Microindentation experiments on the glandular surface. (A) Force–time curve indicating that the material of the plant sample exhibited visco-elastic properties. Pitcher surface was loaded during the first 15 s (Load), then kept in contact with the upper sample for the next 45 s (Relaxation). (B) The indentation of the sample vs applied force (points). The solid line indicates the fit of the indentation data with the Hertz theory.

increased slightly with an increasing applied force ranging from approximately 300 to 1000 μN ($R^2=0.72$, $F_{1,5}=12.78$, $P=0.01$; Fig. 9B; point chosen as an example among six others) or remained constant ($R^2=0.006$, $F_{1,8}=0.05$, $P=0.84$; Fig. 9C; point chosen as an example among two others). Points with

Table 1. Effects of applied force (F_n), plant and point of application on adhesion force

Source	GLM				
	d.f.	SS	MS	F	P
F_n	1	13 304.65	13 304.65	23.29	0.0001
Plant	2	72 386.21	36 193.10	63.37	0.0001
Point (plant)	5	9 719.21	1 943.84	3.40	0.0118
$F_n \times \text{plant}$	2	1 673.71	836.86	1.47	0.2432
$F_n \times \text{point (plant)}$	5	20 485.17	4 097.03	7.16	0.0001

Results of the nested general linear model (GLM; $r^2=0.99$, $F_{21,40}=172.89$, $P=0.0001$), using SAS errors of type 3. d.f., degrees of freedom; F , the ANOVA test statistics; MS, mean square; P , probability value; r^2 , coefficient of determination; SS, sum of squares.

adhesion differed in tenacity from 1.39 to 28.24 kPa. Data on adhesion force and tenacity were not normally distributed and skewed to the left (skewness for adhesion was 1.74 and for tenacity was 1.76), because of the numerous points without adhesion (Fig. 10). There were considerably more points with weak adhesion (adhesion force up to 400 μN , tenacity up to 15 kPa) than with strong adhesion (adhesion force 500–650 μN ; tenacity 22–28 kPa) (Fig. 10). No points with intermediate adhesive properties were found. Hence, points with strong adhesion were probably randomly situated directly on the digestive glands, while points with poor adhesion were located in the vicinity of glands.

Surface free energy

In all three pitchers studied, the glandular surface was readily wetted with all three liquids (Table 2). Contact angles of both polar liquids – water (surface tension= 72.1 mN m^{-1} , dispersion component= 19.9 mN m^{-1} , polar component= 52.2 mN m^{-1} ; Busscher et al., 1984) and ethylene glycol (surface tension= 48.0 mN m^{-1} , dispersion component= 29.0 mN m^{-1} , polar component= 19.0 mN m^{-1} ; Erbil, 1997) – were similar and

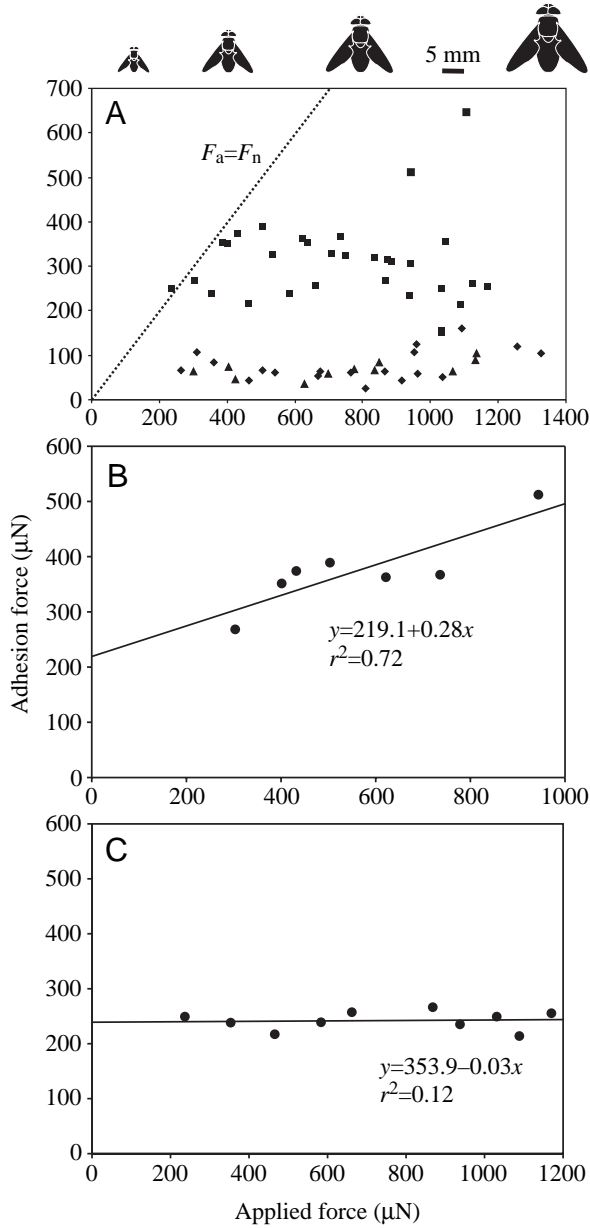


Fig. 9. Dependence of the adhesion force on load. (A) Data of all points on three pitchers. Different symbols correspond to different pitchers. (B,C) Values measured on the same point (selected examples) with increasing applied force. In six out of eight cases, the adhesion increased significantly linearly with the applied force (B), while it remained constant for the other two cases (C). F_a , adhesion force; F_n , applied force.

significantly lower than that of disperse diiodomethane (surface tension = 50.0 mN m^{-1} , dispersion component = 47.4 mN m^{-1} , polar component = 2.6 mN m^{-1} ; Busscher et al., 1984) (one-way ANOVA, $F_{2,37} = 8.934$, $P < 0.001$; Table 3). On the external pitcher surface, the difference between contact angles of all three liquids was highly significant (one-way ANOVA, $F_{2,38} = 48.069$, $P < 0.001$; Table 3). All liquids wetted this surface; however, the contact angle of water was relatively high, especially compared with that on the glandular surface (Tables 2, 3).

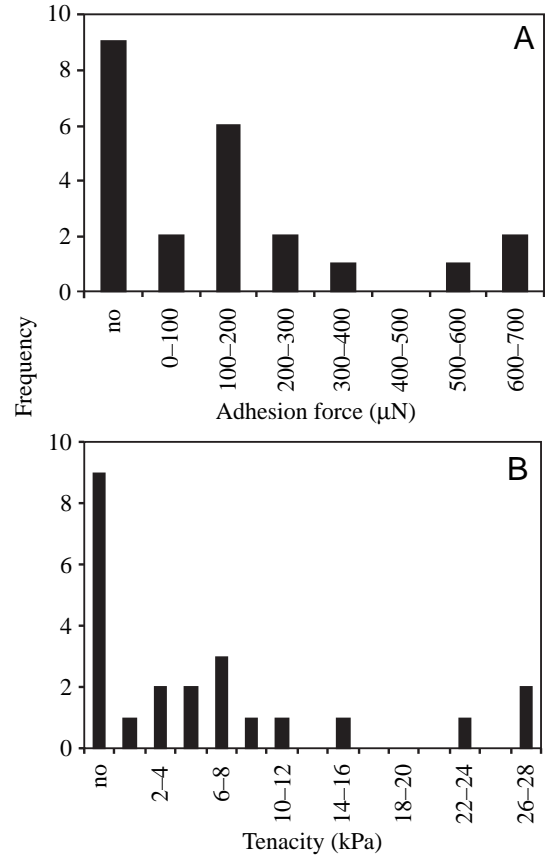


Fig. 10. Frequency histograms of the distribution of points with different values of the adhesion force (A) and the tenacity (B). Only the value of the first test at each point was taken into account.

The glandular surface has a higher surface energy than the external surface of the pitcher, the difference being highly significant and independent of the calculation method used (paired t -test, d.f. = 5, $t = 11.284$, $P < 0.001$). The surface energy calculated for the glandular surface according to two methods had similar total values (one-way ANOVA, $F_{1,4} = 0.113$, $P = 0.753$) but different values of its polar and dispersion components. According to the Owens–Wendt–Kaelble method, the polar component was very high, exceeding the dispersion component by a factor of 3–6 (Table 2). According to the Wu method, both components contributed almost equally to the surface energy: the polar component exceeded the dispersion component only by one-third (Table 2). For the external surface, values of the total surface energy were different depending on the method of calculation (one-way ANOVA, $F_{1,4} = 11.435$, $P = 0.028$). The dispersion component, with one exception, was either slightly or up to twice as high as the polar component (Table 2).

Morphology of the attachment systems of the bug Pyrrhocoris apterus and the fly Calliphora vicina

The tarsus of *Pyrrhocoris apterus* has three segments, which

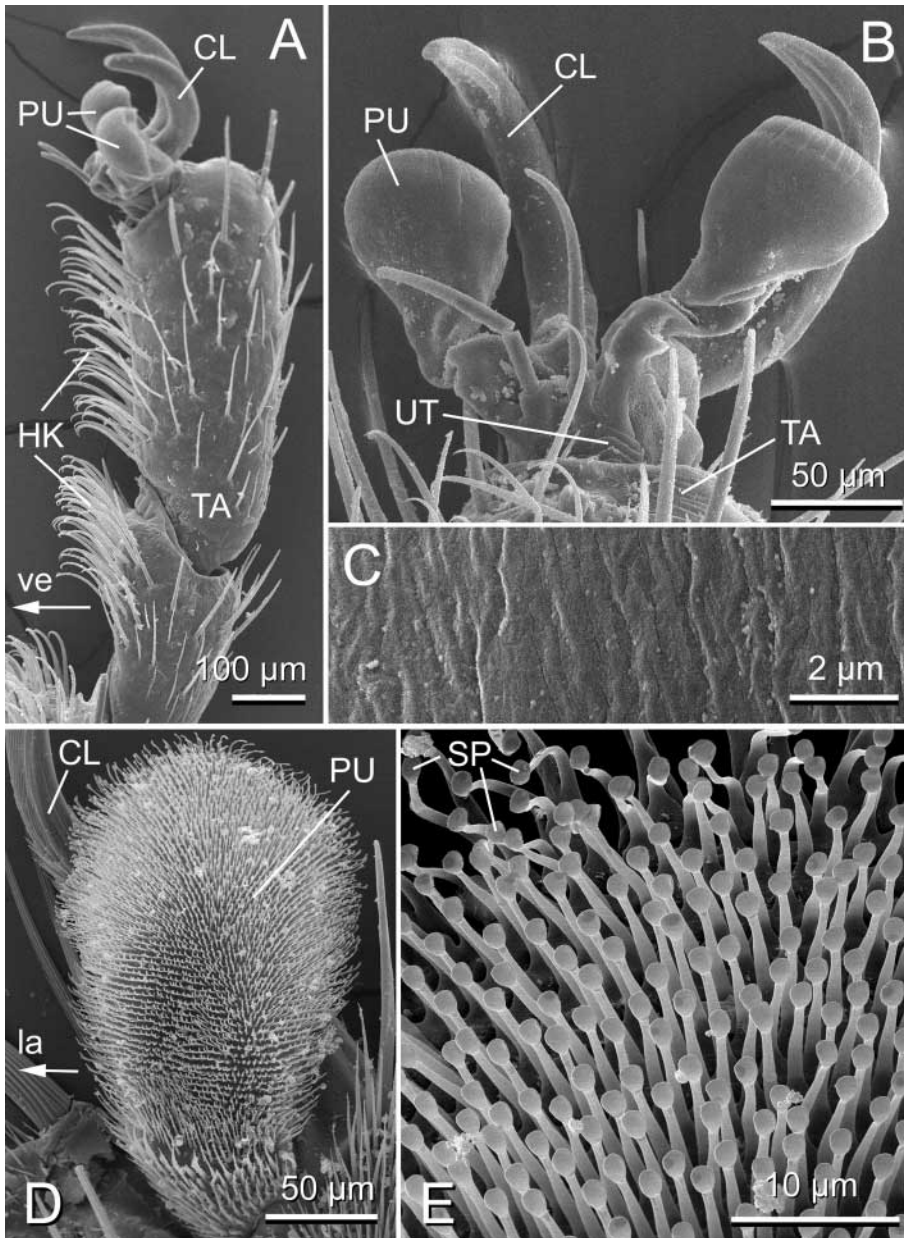


Fig. 11. Attachment devices of insect species studied. (A–C) Smooth pulvilli of the bug *Pyrrhocoris apterus*. (A) Distal part of the tarsus, lateral aspect. (B) Pretarsus, ventral aspect. (C) Surface of the pulvillus. (D,E) Hairy pulvilli of the fly *Calliphora vicina*. (D) Right pulvillus. (E) Tenent setae with the terminal elements (spatulae). CL, claws; HK, hooked setae; la, lateral direction; PU, pulvilli; SP, spatulae; TA, terminal tarsomere; UT, unguitactor plate; ve, ventral direction.

Friction force generated by insects on the glandular surface

Values of the maximal friction force generated by insects differed significantly according to the substrate studied, the insect species and the individual for a given species and a given substrate (Table 4). Moreover, the substrate influenced the performance of insects differently according to whether they were bugs or flies (interaction species \times substrate, significant). For example, on a fresh glandular surface, the friction force generated by bugs was reduced compared with glass, while it was enhanced for flies.

Effect of substrate

The effect of substrate on insect performance was the most significant effect (Table 4). For the bug *Pyrrhocoris apterus*, the highest force was measured on a dry glandular surface, and the lowest one was measured on a fresh glandular surface (Fig. 12A). The fly *Calliphora vicina* showed the highest friction force on

are ventrally covered with hooked setae, curved proximally (Fig. 11A). The pretarsus bears two pulvilli connected to the pretarsus in the region between the unguitactor plate and claws. Pulvilli appear rather smooth in SEM images (Fig. 11B); however, slight corrugation of the surface may be observed at a high magnification (Fig. 11C). Pulvilli material seems to be very compliant and it collapses in air-dried samples.

The tarsus of *Calliphora vicina* has five segments, ventrally covered with setae, pointed proximally. The pretarsus bears two pulvilli connected to claws through mobile sclerites called auxilia. The pulvilli are densely covered with tenent setae (Fig. 11D). Each seta is composed of a shaft (15–20 μm long) and a terminal plate, or spatula (1.5–2.0 μm wide) (Fig. 11E).

both glandular substrates and performed much worse on glass (Fig. 12A). There was no significant difference in the flies' performances on the fresh or dry states of the glandular surface, whereas the force on glass differed significantly from both glandular surfaces (Table 4; Fig. 12A). SEM observation of insects immediately killed after the experiments clearly demonstrated that pitcher secretion did not contaminate the pads of either insect studied.

Differences between insects

Insect species studied showed significant difference in maximal friction force on all three substrates tested (Fig. 12B). On both glass and dry glandular surfaces, bugs produced a higher friction force than flies, while on fresh glandular surfaces flies performed better (Fig. 12B).

Table 2. Contact angles of three liquids on the glandular surface of the digestive zone and the external surface of the pitcher, and free surface energy (total and its dispersion and polar contributions) of the surfaces calculated according to the Owens–Wendt–Kaelble method (OW) and the Wu method (W)

Plant	Liquid	Contact angle (deg.)		Surface energy OW (mN m ⁻¹)			Surface energy W (mN m ⁻¹)		
		Mean ± s.d.	<i>n</i>	Total	Dispersion	Polar	Total	Dispersion	Polar
Glandular surface									
1	Water	36.7±1.2	3	56.84	12.62	44.41	56.98	24.05	32.93
	Diiodomethane	50.6±2.8	3						
	Ethylene glycol	40.0±0.8	3						
2	Water	30.0±5.3	5	60.80	15.90	44.90	61.93	28.85	33.09
	Diiodomethane	36.0±4.6	5						
	Ethylene glycol	32.7±6.1	5						
3	Water	31.9±4.6	5	61.57	8.87	52.70	58.19	21.68	36.51
	Diiodomethane	54.7±11.4	5						
	Ethylene glycol	43.3±10.9	5						
External surface									
1	Water	70.5±0.2	3	38.09	26.08	12.01	43.59	31.36	12.23
	Diiodomethane	39.5±3.9	4						
	Ethylene glycol	48.8±11.3	4						
2	Water	59.3±4.5	5	41.76	19.24	22.52	46.67	28.13	18.54
	Diiodomethane	42.0±2.5	5						
	Ethylene glycol	50.7±2.3	5						
3	Water	62.2±9.2	5	41.34	21.60	19.74	46.83	29.77	17.06
	Diiodomethane	40.5±2.3	5						
	Ethylene glycol	45.5±5.4	5						

n, number of measurements.

Table 3. Results of multiple comparison of means (Tukey test) carried out in ANOVA for contact angles of diiodomethane, ethylene glycol and water to the glandular surface and external pitcher surface

Comparison	DM	<i>p</i>	<i>Q</i>	<i>P</i>
Glandular surface				
Diiodomethane vs water	14.300	3	5.360	<0.001
Diiodomethane vs ethylene glycol	8.584	3	3.629	0.038
Ethylene glycol vs water	5.716	3	2.416	0.216
External surface				
Diiodomethane vs water	22.257	3	13.677	<0.001
Ethylene glycol vs water	14.714	3	9.042	<0.001
Diiodomethane vs ethylene glycol	7.543	3	4.724	0.005

DM, difference of means; *p*, number of means spanned in the comparison; *P*, probability value; *Q*, test statistics.

Discussion

In *Nepenthes* plants, the digestive zone has large multicellular glands that develop from single epidermal cells (Owen and Lennon, 1999). The zone might be completely or partly filled by digestive liquid (Juniper et al., 1989). The digestive fluid contains enzymes, such as proteases and

Table 4. Effects of surface, insect species and individual on the friction force generated by insects

Source	Three-way ANOVA				
	d.f.	SS	MS	<i>F</i>	<i>P</i>
Species	1	27.95	27.95	10.42	0.0016
Substrate	2	152.77	76.39	28.47	0.0001
Species × substrate	2	268.04	134.02	49.96	0.0001
Individual (species × substrate)	24	837.69	36.40	13.57	0.0001

Results of the three-way ANOVA ($r^2=0.81$, $F_{29,119}=17.06$, $P=0.0001$), using SAS errors of type 3. d.f., degrees of freedom; *F*, the ANOVA test statistics; MS, mean square; *P*, probability value; r^2 , coefficient of determination; SS, sum of squares.

chitinases, organic acids, chlorine and sodium ions and water, produced by glands, and serves for trapping and breaking up the prey (Juniper et al., 1989; Owen and Lennon, 1999). In contrast to most plant glands, those of the digestive zone have not one but several functions, and their role was found to be developmentally regulated (Owen and Lennon, 1999; Owen et al., 1999). Prior to pitcher maturity, they supply the pitcher with fluid, i.e. they secrete several groups of molecules. At maturity, secretion is blocked, and the main function is the absorption of prey-derived nutrients.

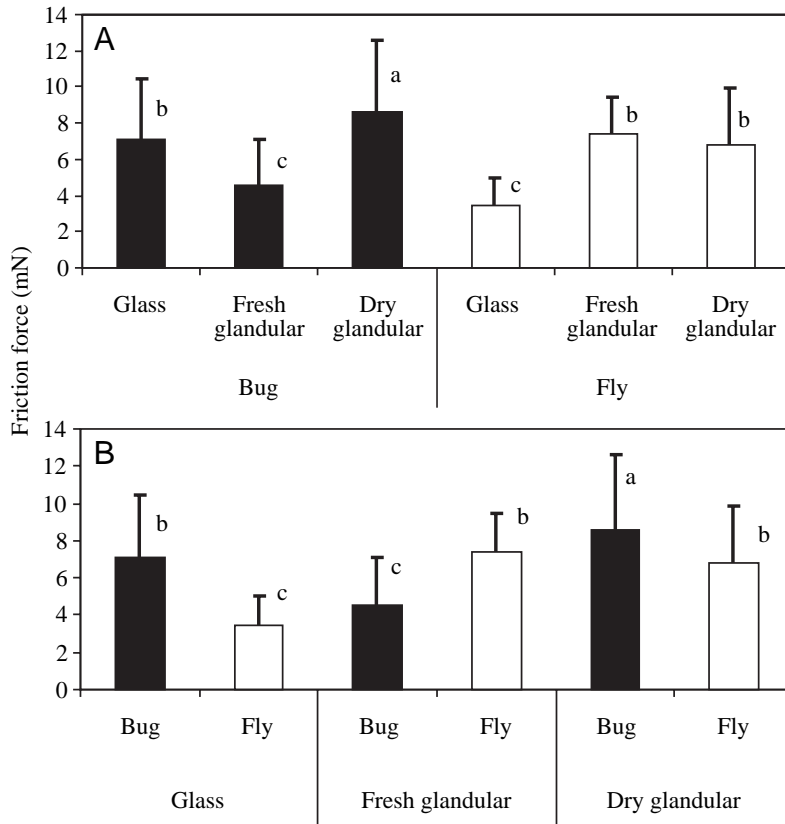


Fig. 12. Maximal friction force generated by insects on different substrates. (A) Comparison between three surfaces tested. (B) Comparison between two insect species. According to the Ryan–Eliot–Gabriel–Welsh test of multiple comparisons of means, run after ANOVA, means with different letters differ significantly from each other.

Once an animal is captured in the digestive fluid, it may struggle in the liquid and succeed in leaving the pool and try to escape. It was previously indicated that, as well as all other functional pitcher surfaces, the glandular surface displays properties responsible for the retention of insects within the pitcher (Gaume et al., 2002). However, the possible role of the glandular surface, the glands or the gland secretion in the trapping and retaining system of the pitcher has not been fully elucidated.

Our data on the morphology, material and surface properties of the glandular surface and the experimental results obtained in friction tests with two insect species provide a good basis for discussing the possible anti-attachment function of the glandular zone and the mechanism of trapping in general.

Possible role of surface morphology in preventing insect attachment

Our results on the morphology and surface profile showed that the glandular surface is not uniform and smooth but bears structures causing significant roughness of the surface. Surface roughness results from (1) epidermal depressions (up to 30 μm deep) with glands placed at the bottom, (2) prominent hoods (15–30 μm high) overhanging the upper margins of depressions and (3) prominent sessile glands (up to 15 μm high) that do not extend beyond depressions (in the upper and middle part of the digestive zone) or protrude out of the epidermal surface to a depth of no more than one half of the height of the gland (in the lower part of the zone). The presence

of depressions, containing digestive glands, and hoods has been previously described in other *Nepenthes* species (Lloyd, 1942; Adams and Smith, 1977; Pant and Bhatnagar, 1977; Juniper et al., 1989; Owen and Lennon, 1999; Owen et al., 1999; Gaume et al., 2002). Towards the bottom of the pitcher, the dimensions and prominence of hoods decrease, whereas those of glands increase, so that the surface becomes increasingly uneven.

Prevention of claw interlocking

It is known that insects attach well to a macroscopically rough surface (Dai et al., 2002; Betz, 2002). In this case, insects usually use surface irregularities as anchorage sites for their claws (Nachtigall, 1974; Cartmill, 1985). It has been previously shown that insects having tarsi equipped only with claws are able to attach to vertical substrates only if the diameter of surface asperities

is much larger than the diameter of the claw tips (Dai et al., 2002). In *N. ventrata*, the size of depressions, hoods and glands greatly exceeds claw tip diameter (1–5 μm depending on insect size), therefore the rough-structured glandular pitcher surface can guarantee a sufficient number of sites for successful claw interlocking for insects.

However, the geometrical features of some structures covering the glandular surface may prohibit the use of large surface asperities for clinging. Firstly, pendant hoods covering either both the upper slope and the central region in upper glands or only the upper slope of glands (in the lower part of the zone) not only protect gland cells from being scraped by insect feet but may also prevent insects from clinging to both hoods and glands (Lloyd, 1942; Juniper et al., 1989). Moreover, anisotropic hoods may induce insects to fall and impede their escape in a similar way as the downward-directed lunulate cells of the waxy zone in *N. alata* (Lloyd, 1942; Gaume et al., 2002). Secondly, depressions with the angle of slope in a proximal direction of the pitcher may preclude insects from using them as foot-holds. However, in the lower part of the digestive zone and particularly at the bottom of the pitcher, the surface roughness increases and the anisotropy of the surface profile almost disappears. Interestingly, this probably does not affect the retaining function of the glandular surface because, as in mature pitchers, the lower regions of the glandular surface are usually submerged in the pool of digestive fluid (Juniper et al., 1989; Owen and Lennon, 1999; Owen et al., 1999).

Attachment by means of adhesive pads

In order to attach to smooth substrates, many insects have evolved specialised adhesive pads based on two different mechanisms: smooth flexible pads and hairy structures (Gorb, 2001). Compliant pad material in the first case and fibrillar surface structures in the second guarantee to maximise the contact area and ensure a high attachment force on smooth substrates (Gorb, 2001; Beutel and Gorb, 2001). It has been previously reported that many insects showed excellent attachment ability on a variety of smooth artificial and natural substrates (Way and Murdie, 1965; Stork, 1980; Edwards, 1982; Eigenbrode, 1996; Eigenbrode et al., 1999; Federle et al., 2000). An experimental study of the attachment ability of the beetle *Chrysolina fastuosa* (Chrysomelidae), possessing claws and hairy adhesive pads, on various plant substrates revealed successful attachment to 46 smooth surfaces of 41 plant species (Gorb and Gorb, 2002). The presence of cellular sculpturing, sinuous fissures and additional subcellular irregularities on these surfaces did not lessen the attachment. It was suggested that on smooth substrates, even if they are not perfectly smooth, the area of real contact between the substrate and the terminal elements of the beetle is large enough to provide a high attachment force. In the digestive zone of the *N. ventrata* pitcher, the surface between glands has a smooth appearance and is slightly uneven due to low convexities. The effect of various smooth plant substrates on insect attachment (Gorb and Gorb, 2002) may also be extended to the glandular surface of *Nepenthes*. This surface could provide appropriate substrate for insect attachment in the case of pad-bearing insects. The surface of the glands, although slightly corrugated and covered with tiny scale-like subcellular asperities, may also present a proper support for adhesive pads.

Mechanical strength of the surface

Anatomical study of the epidermal surface and glands of the digestive zone revealed no specialised structures that could influence insect attachment. Nevertheless, some features of the inner morphology may contribute to the enhancement of the pitcher wall rigidity resisting external forces from insects attempting to cling to the glandular surface. The surface between the glands is covered by epidermal cells with thick lateral and greatly thickened outer walls. The glandular head cells also have thicker lateral walls and an extremely thick external wall. It has been previously hypothesised for the carnivorous plant *Sarracenia purpurea* that the thick lateral walls in the epidermal cells of the absorption zone may reinforce the pitcher against struggling prey (Barckhaus and Weinert, 1974). The same function may also be suggested for the glandular surface of *Nepenthes* plants. Moreover, cutin impregnations in these thick external cell walls in the epidermis, epidermal ridges and glandular head cells, indicated from UV fluorescence, contribute not only to the formation of a barrier to apoplastic transport (Juniper et al., 1989; Owen and Lennon, 1999) but also may contribute to an increase in the mechanical strength of the glandular surface. Besides the cutinised wall layer, the surface between glands and the gland

surface itself are covered with a cuticle layer, relatively thick in the first case and very thin on the glands. The presence of the thick cuticle that covers the epidermis and extends over the top of the digestive glands was also found in *N. alata* pitchers (Owen and Lennon, 1999). Using our microscopy methods, cuticular gaps, reported as characteristic cuticular discontinuity in glands of *Nepenthes*, *Drosophyllum*, *Sarracenia* and *Utricularia* (reviewed by Juniper et al., 1989), were not detected in *N. ventrata*.

Mechanical properties of the digestive zone and insect retention

It was previously suggested that the pitcher wall in *Nepenthes* is extremely strong owing to the thick-walled epidermis of the outer and inner surfaces, as well as mechanical reinforcement by heavily sclerenchymatised veins and non-vascular idioblasts (Lloyd, 1942; Juniper et al., 1989). This strengthening was believed to prohibit escape through the sides of the pitcher by leaf-cutting insects, that was sometimes observed in representatives of several genera of carpenter wasps. However, the material properties of the pitcher wall and the surface properties of its inner surface have not been previously estimated, although these parameters may be important for trapping and retaining.

The results of microindentation experiments on the glandular surface allow us to conclude that the material of the inner surface in the digestive zone has visco-elastic properties. However, taking into account the relatively low load forces, which insects may apply to this substrate, the system of the plant pitcher wall may be considered to function mainly in the elastic regime. For this reason, in our estimations, we neglected, as less important for insect-retention, the viscous component of the material properties of the plant tissue studied.

Effect of surface material stiffness on insect attachment

Previous authors have shown that substrate stiffness as well as the diameter of surface asperities may influence the friction force of the tarsal claw system (Dai et al., 2002). In order to allow insect attachment and locomotion, elements of the surface roughness should be greater in dimension than the claw tip diameter, and the substrates should be sufficiently stiff to prevent its penetration by claws, otherwise the claws will slide over the surface. As was shown above, despite appropriate roughness, the glandular surface does not appear to allow effective claw interlocking because of the surface anisotropy such as the direction and orientation of structures such as the hooded epidermal cells and the proximally sloped surfaces of gland depressions.

In terms of surface stiffness, claw clinging might be possible due to indentations formed by 'punching' the surface, *via* forces applied by the claws. In this case, the stiffness of the substrate may play a crucial role in providing a sufficient attachment force.

We estimated whether the glandular surface could have accommodated claw attachment *via* a 'punching' process. On

the basis of the microindentation experiments, the Young's modulus of the material in the digestive zone was found to be 637.19 kPa. It is known that insect claws are made of a hard cuticle that was reported to have a Young's modulus of ~9 GPa (Neville, 1975). We assumed that insects can attach to the surface and move on it if the claws make deep dents, which noticeably exceed the diameter of the claw tip. To each claw, the insect applies a force equal to its weight divided by 12, when all six legs are used in attachment; during locomotion, this weight is divided by six, when only three legs are in contact with the substrate. According to the Hertz model (Hertz, 1881), light insects (3 mg) possessing claws with a tip diameter of 1 μm indent the surface to a depth of 2.14 μm (using six legs) or 3.39 μm (using three legs). For heavier insects (300 mg) with a claw tip diameter of 5 μm , the dents are 26.91 μm (for six legs) and 42.72 μm (for three legs) deep. Thus, in cases of small and relatively larger insects relevant to the plant species studied, the depth of dents made by claws is much larger than the claw tip diameter. In summary, this indicates that the glandular surface can guarantee claw interlocking if the required surface roughness is lacking.

To obtain strong attachment, using adhesive pads, a large contact area between the surface and the pads is required in order to achieve a strong attracting force. For this purpose, materials of either or both contacting bodies should be very compliant. In insects having a smooth type of attachment device, a very low stiffness of pad material (Young's modulus 27.2 ± 11.6 kPa) coupled with a specific ultrastructural architecture of the cuticle have been previously found (Gorb et al., 2000). This type of cuticle architecture allows surface replication and thus an increase of the area of real contact between a substrate and the pad. Insects with hairy adhesive pads were reported to be able to replicate the substrate profile not only due to the division of one large contact into many small ones (Scherge and Gorb, 2001; Arzt et al., 2003) but also because of the high flexibility of terminal elements called tenent setae (spring constant 1.31 N m^{-1} ; Niederregger et al., 2002). Our microindentation experiments showed that the material of the digestive zone is relatively stiff. This means that it is not the plant tissue, but the adhesive pads, that contribute mostly to an increased contact area between these surfaces.

Influence of surface adhesive properties on insect attachment and locomotion

Another mechanism contributing to the attachment strength is the adhesive energy of the contacting surfaces. It is known that pad-bearing insects deliver secretory fluid onto the contact zone to increase the attachment force between the pad and the substrate (Ishii, 1987; Kosaki and Yamaoka, 1996; Gorb, 1998; Eisner and Aneshansley, 2000; Voetsch et al., 2002; Federle et al., 2002). Insects are thus able to increase the capillary and viscous forces contributing to overall adhesion. For insects without adhesive pads, attachment to smooth surfaces may only be possible because of specific properties of the substrate. In our further estimations, we discuss the possible effect of the glandular surface on the adhesion of pad-less insects.

Adhesive properties of the glandular surface are very inhomogeneous. There are many non-adhesive areas that cannot accommodate insect attachment. The adhesive areas also vary greatly in values of measured adhesion force. Most adhesive points showed a weak adhesion force and low tenacity. To estimate whether this adhesion is sufficient to guarantee the insects attachment, we performed the following calculation. In order for small and middle-sized insects (up to 40 mg) to adhere to a substrate with all six legs having an approximate contact area of $8000 \mu\text{m}^2$ per leg (estimated for insects used in this study), a surface tenacity of at least 5 kPa is required. In order for the plant surface to accommodate locomotion, when only three legs are in contact with the substrate, a tenacity of at least 10 kPa would be required. To fulfil this, all the attachment structures should contact the substrate areas with these adhesive properties. However, a tenacity of more than 10 kPa was actually found to be rather rare on the glandular surface. Therefore, if insects do not use specialised adhesive organs, this surface cannot provide sufficient adhesion for insect attachment. For heavier insects with the same contact area, a higher substrate tenacity is required for adherence to the glandular surface (Fig. 9A). Although very few points with strong adhesion and high tenacity (22–28 kPa) were also found, they were not believed to be significant for the effective attachment and locomotion for large insects but may function as solitary adhesive spots that glue small insects and impede their locomotion (Gaume et al., 2002). This may limit their escape potential from the trap.

We found that the adhesion force increased at a lower rate than the load (Fig. 9A,B, slope < 1). Thus, lighter insects should adhere relatively more strongly than heavier insects. Moreover, in nature, the surface is vertical and heavier insects will have a greater disadvantage due to their weight, which tends to pull them inside the pitcher. This may support the idea that light insects can attach to the glandular surface without using specialised adhesive organs if the surface adhesion exceeds the insect weight (Fig. 9A; points located on the left side of the line $F_a = F_n$).

Physico-chemical properties of the surface and pad adherence

Surface free energy of the substrate is another important parameter affecting adhesion between two contacting bodies. It is known that, in solids, surface energy plays a crucial role in contact, since it leads to an increase of the real contact area, which results in a high attracting force (Israelachvili, 1992). In contrast to other pitcher surfaces, the glandular surface has a rather high surface free energy. This must ensure a high adhesion force based on the capillary interaction. Moreover, the polar component of the surface energy greatly exceeded the dispersal component. As the polar component demonstrates the presence of far-ranging forces, this surface will additionally contribute to attractive interaction between contacting bodies (Israelachvili, 1992). The glandular surface was found to be hydrophilic (strong attractive interaction between the surface and water). The pad secretion produced by insects has been

reported to contain oily substances (Ishii, 1987; Kosaki and Yamaoka, 1996; Eisner and Aneshansley, 2000). Recent work has further demonstrated the presence of water and water-soluble substances in pad secretion (Gorb, 2001; Voetsch et al., 2002; Federle et al., 2002). Therefore, it may be assumed that on the hydrophilic glandular surface, the polar water component of the pad secretion contributes substantially to adhesion, in addition to the disperse oily component. Thus, both components of the pad secretion can probably promote an increase of capillary forces that provides successful insect attachment on the glandular surface of the pitcher.

Attachment of insects with different pad design to the glandular pitcher surface

Our results showed that the bug *Pyrrhocoris apterus*, having a smooth attachment system, generated a significantly lower friction force on the fresh glandular surface than on a smooth dry glass plate used as a reference substrate. However, on the air-dried glandular surface, the force was higher than on both glass and fresh glandular surfaces. This indicates that the gland secretion on a fresh plant surface reduces the attachment force. We assume that the gland secretion does not function as a glue, as was previously hypothesised (Gaume et al., 2002). Rather, the gland secretion may increase the thickness of the fluid layer between the pad surface and the substrate. This causes a lubrication effect in the contact between surfaces and decreases friction force. In other words, the substrate becomes slippery. On the fresh glandular surface, bugs were able to use their claws to interlock to surface irregularities, since the surface anisotropy was probably not as effective with the plant sample placed horizontally. The highest friction force obtained on the dry glandular surface may be explained by the use of both adhesive pads to attach to smooth areas between glands and claws to cling to macro-asperities of the substrate.

The fly *Calliphora vicina*, having a hairy attachment system, performed equally well on both fresh and air-dried glandular surfaces and much worse on the glass plate. This indicates that on the glandular surface, insects presumably used both claws and adhesive pads, whereas on glass, only pads were used for attachment. In contrast to the smooth pads of bugs, the hairy pads of flies were not disabled by the gland secretion. Superfluous fluid, occurring on the glandular surface, probably fills the spaces between tenent setae and therefore did not affect the friction force through lubrication.

A comparison of the performance of the two insect species on glass showed that bugs generated a significantly higher force than flies. The same trend was also found on the dried glandular substrate. This means that on dry substrates, using either adhesive pads or both pads and claws in the attachment, both smooth and hairy structures succeed. However, on the fresh plant surface, flies showed a significantly higher friction force. In this case, not only claws but also pads seemed to contribute to the generation of a friction force. Thus, we assume that the presence of the additional layer of fluid in a contact zone may disable smooth adhesive pads, whereas it does not worsen the effectiveness of hairy systems. This might

be explained by the fact that in the hairy system, superfluous fluid may be drawn off into intersetal spaces. The secretion does not appear to contaminate either type of adhesive pads.

Concluding remarks

This study represents a complex investigation of plant–insect surface interactions, including general morphology, internal structure, material and adhesive properties, and surface energy in the highly specialised glandular tissue of *Nepenthes*. The study is also combined with measurements of attachment forces generated by insects on this plant surface. On the basis of structural, physico-chemical and mechanical characterisation of the plant surface, we tried to estimate the possible functional importance of the glandular surface in the trapping and retaining mechanism of *N. ventrata*. We assume that the influence of the plant surface on insect attachment differs depending on insect weight and design of their attachment systems. In general, the glandular surface is probably not responsible for prey capture and retention.

List of symbols and abbreviations

A	contact area
a	radius of the circular contact area
E	Young's modulus of the plant sample
E_b	Young's modulus of the sapphire sphere
F_a	adhesive force
F_n	applied force
K	reduced elasticity modulus of materials
N	number of pitchers
n	number of samples or measurements
R	sapphire sphere radius
T	tenacity
δ	indentation
ν	Poisson ratio of the plant sample
ν_b	Poisson ratio of the sapphire sphere

Sincere thanks to Y. Jiao (Simon Fraser University, Burnaby, Canada) for his help in evaluation of the Young's modulus and tenacity. Discussions with S. Enders (MPI for Metals Research, Stuttgart, Germany) on estimation of the modulus of elasticity of the plant material are acknowledged. We thank J. Berger (Electron Microscopy Unit at the MPI of Developmental Biology, Tübingen, Germany) for permanent support. K. Scheller (University of Würzburg, Germany) kindly supplied *Calliphora vicina*. This work was supported by the Federal Ministry of Education, Science and Technology, Germany to S.G. (Project BioFuture 0311851).

References

- Adams, R. M and Smith, G. W. (1977). An SEM survey of the five carnivorous pitcher plant genera. *Am. J. Bot.* **64**, 265-272.
- An, C.-I., Fukusaki, E.-I. and Kobayashi, A. (2001). Plasma-membrane H⁺-ATPases are expressed in pitchers of the carnivorous plant *Nepenthes alata* Blanco. *Planta* **212**, 547-555.

- Arzt, E., Gorb, S. and Spolenak, R. (2003). From micro to nano contacts in biological attachment devices. *Proc. Natl. Acad. Sci. USA* **100**, 10603-10606.
- Barrckhaus, R. and Weinert, H. (1974). Die fleischfressende Pflanze *Sarracenia purpurea*: Licht- und elektronenmikroskopische Untersuchungen. *Mikrokosmos* **63**, 38-47.
- Bauchhenss, E. (1979). Die Pulvillen von *Calliphora erythrocephala* Meig. (Diptera, Brachycera) als Adhäsionsorgane. *Zoomorphologie* **93**, 99-123.
- Betz, O. (2002). Performance and adaptive value of tarsal morphology in rove beetles of the genus *Stenus* (Coleoptera, Staphylinidae). *J. Exp. Biol.* **205**, 1097-1113.
- Beutel, R. and Gorb, S. N. (2001). Ultrastructure of attachment specialization of hexapods (Arthropoda): evolutionary patterns inferred from a revised ordinal phylogeny. *J. Zool. Syst. Evol. Res.* **39**, 177-207.
- Busscher, H. J., Vanpert, A. W. J., Deboer, P. and Arends, J. (1984). The effect of the surface roughening of polymers on measured contact angle of liquids. *Coll. Surf.* **9**, 319-331.
- Cartmill, M. (1985). Climbing. In *Functional Vertebrate Morphology* (ed. M. Hildebrand, D. N. Bramble, K. F. Liem and D. B. Wake), pp. 73-88. Cambridge: The Belknap Press.
- Clarke, C. (2001). *Nepenthes of Sumatra and Peninsular Malaysia*. Kota Kinabalu, Malaysia: Natural History Publications (Borneo).
- Dai, Z., Gorb, S. and Schwarz, U. (2002). Roughness-dependent friction force of the tarsal claw system in the beetle *Pachnoda marginata* (Coleoptera, Scarabaeidae). *J. Exp. Biol.* **205**, 2479-2488.
- Edwards, P. B. (1982). Do waxes of juvenile *Eucalyptus* leaves provide protection from grazing insects? *Austr. J. Ecology* **7**, 347-352.
- Eigenbrode, S. D. (1996). Plant surface waxes and insect behaviour. In *Plant Cuticles – an Integral Functional Approach* (ed. G. Kerstiens), pp. 201-222. Oxford: BIOS.
- Eigenbrode, S. D., Kabalo, N. N. and Stoner, K. A. (1999). Predation, behavior, and attachment by *Chrysoperla plorabunda* larvae on *Brassica oleracea* with different surface waxblooms. *Entomol. Exp. Appl.* **90**, 225-235.
- Eisner, T. and Aneshansley, D. J. (2000). Defence by foot adhesion in a beetle (*Hemisphaerota cyanea*). *Proc. Natl. Acad. Sci. USA* **97**, 6568-6573.
- Erbil, H. Y. (1997). Surface tension of polymers. In *CRC Handbook of Surfaces and Colloid Chemistry* (ed. K. S. Birdi), pp. 265-312. Boca Raton: CRC Press Inc.
- Federle, W., Rohrseitz, K. and Hölldobler, B. (2000). Attachment forces of ants measured with a centrifuge: better "wax-runners" have a poorer attachment to a smooth surface. *J. Exp. Biol.* **203**, 505-512.
- Federle, W., Riehle, M., Curtis, A. S. G. and Full, R. J. (2002). An integrative study of insect adhesion: mechanics and wet adhesion of pretarsal pads in ants. *Integr. Comp. Biol.* **42**, 1100-1106.
- Gaume, L., Gorb, S. and Rowe, N. (2002). Function of epidermal surfaces in the trapping efficiency of *Nepenthes alata* pitchers. *New Phytol.* **156**, 476-489.
- Gaume, L., Perret, P., Gorb, E., Gorb, S. and Rowe, N. (2004). How do plant waxes cause flies to slide? Experimental tests of wax-based trapping mechanisms in three pitfall carnivorous plants. *Arthropod Struct. Develop.* **33**, 103-111.
- Gorb, S. N. (1998). The design of the fly adhesive pad: distal tenent setae are adapted to the delivery of an adhesive secretion. *Proc. R. Soc. Lond. B* **265**, 62-70.
- Gorb, S. N. (2001). *Attachment Devices of Insect Cuticle*. Dordrecht, Boston, London: Kluwer Academic Publishers.
- Gorb, S. N. and Beutel, R. G. (2001). Evolution of locomotory attachment pads of hexapods. *Naturwissenschaften* **88**, 530-534.
- Gorb, E. V. and Gorb, S. N. (2002). Attachment ability of the beetle *Chrysolina fastuosa* on various plant surfaces. *Entomol. Exp. Appl.* **105**, 13-28.
- Gorb, S. N. and Popov, V. L. (2002). Probabilistic fasteners with parabolic elements: biological system, artificial model and theoretical considerations. *Phil. Trans. R. Soc. Lond. A* **360**, 211-225.
- Gorb, S., Jiao, Y. and Scherge, M. (2000). Ultrastructural architecture and mechanical properties of attachment pads in *Tettigonia viridissima* (Orthoptera, Tettigoniidae). *J. Comp. Physiol. A* **186**, 821-831.
- Gorb, S., Gorb, E. and Kastner, V. (2001). Scale effects on the attachment pads and friction forces in syrphid flies (Diptera, Syrphidae). *J. Exp. Biol.* **204**, 1421-1431.
- Hasenfuss, I. (1977). Die Herkunft der Adhäsionsflüssigkeit bei Insekten. *Zoomorphologie* **87**, 51-64.
- Hasenfuss, I. (1978). Über das Haften von Insekten an glatten Flächen – Herkunft der Adhäsionsflüssigkeit. *Zool. Jahrb. Anat.* **99**, 115-116.
- Hertz, H. (1881). Über den Kontakt elastischer Körper. *J. Reine Angewandte Mathematik* **92**, 156-171.
- Ishii, S. (1987). Adhesion of a leaf feeding ladybird *Epilachna vigintioctomaculata* (Coleoptera: Coccinellidae) on a vertically smooth surface. *Appl. Entomol. Zool.* **22**, 222-228.
- Israelachvili, J. (1992). *Intermolecular and Surface Forces*. London: Academic Press.
- Jebb, M. and Cheek, M. (1997). A skeletal revision of *Nepenthes* (Nepenthaceae). *Blumea* **42**, 1-106.
- Jiao, Y., Gorb, S. and Scherge, M. (2000). Adhesion measured on the attachment pads of *Tettigonia viridissima* (Orthoptera, Insecta). *J. Exp. Biol.* **203**, 1887-1895.
- Johnson, K. L., Kendall, K. and Roberts, A. D. (1971). Surface energy and the contact of elastic solids. *Proc. R. Soc. Lond. A* **324**, 301-313.
- Juniper, B. E. and Burras, J. K. (1962). How pitcher plants trap insects. *New Scientist* **13**, 75-77.
- Juniper, B. E., Robins, R. J. and Joel, D. M. (1989). *The Carnivorous Plants*. London: Academic Press.
- Kato, M., Hotta, M., Tamin, R. and Itino, I. (1993). Inter- and intra-specific variation in prey assemblages and inhabitant communities in *Nepenthes* pitchers in Sumatra. *Trop. Zool.* **6**, 11-25.
- Kosaki, A. and Yamaoka, R. (1996). Chemical composition of footprints and cuticula lipids of three species of lady beetles. *Jap. J. Appl. Entomol. Zool.* **40**, 47-53.
- Lloyd, F. E. (1942). *The Carnivorous Plants*. New York: The Ronald Press Company.
- Maier, G. (2002). *Operating Manual DataPhysics OCA*, release 2.0. Filderstadt, Germany.
- Mohsenin, N. N. (1986). *Physical Properties of Plant and Animal Materials*. New York: Gordon and Breach Science Publishers.
- Moran, J. A. (1996). Pitcher dimorphism, prey composition and the mechanism of prey attraction in the pitcher plant *Nepenthes rafflesiana* in Borneo. *J. Ecol.* **84**, 515-525.
- Moran, J. A., Booth, W. E. and Charles, J. K. (1999). Aspects of pitcher morphology and spectral characteristics of six Bornean *Nepenthes* pitcher plant species: implications for prey capture. *Ann. Bot.* **83**, 521-528.
- Nachtigall, W. (1974). *Biological Mechanisms of Attachment*. Berlin, Heidelberg, New York: Springer.
- Neville, A. C. (1975). *Biology of the Arthropod Cuticle*. Berlin, Heidelberg, New York: Springer.
- Niederregger, S., Gorb, S. and Jiao, Y. (2002). Contact behaviour of tenent setae in attachment pads of the blowfly *Calliphora vicina* (Diptera, Calliphoridae). *J. Comp. Physiol. A* **187**, 961-970.
- Niklas, K. J. (1992). *Plant Biomechanics: An Engineering Approach to Plant Form and Function*. Chicago, London: The University of Chicago Press.
- Owen, T. P. and Lennon, K. A. (1999). Structure and development of the pitchers from the carnivorous plant *Nepenthes alata* (Nepenthaceae). *Am. J. Bot.* **86**, 1382-1390.
- Owen, T. P., Lennon, K. A., Santo, M. J. and Anderson, A. Y. (1999). Pathways for nutrient transport in the pitchers of the carnivorous plant *Nepenthes alata*. *Ann. Bot.* **84**, 459-466.
- Owens, D. K. and Wendt, R. C. (1969). Estimation of the surface free energy of polymers. *J. Appl. Polymer Sci.* **13**, 1741-1747.
- Pant, D. D. and Bhatnagar, S. (1977). Morphological studies in *Nepenthes*. *Phytomorphology* **27**, 13-34.
- Scherge, M. and Gorb, S. N. (2001). *Biological Micro- and Nanotribology*. Berlin, Heidelberg, New York: Springer.
- Schulze, W., Frommer, W. B. and Ward, J. M. (1999). Transporters for ammonium, amino acids and peptides are expressed in pitchers of the carnivorous plant *Nepenthes*. *Plant J.* **17**, 637-646.
- Slack, A. (2000). *Carnivorous plants*. Cambridge, MA: MIT Press.
- Stork, N. E. (1980). Experimental analysis of adhesion of *Chrysolina polita* (Chrysomelidae, Coleoptera) on a variety of surfaces. *J. Exp. Biol.* **88**, 91-107.
- Voetsch, W., Nicholson, G., Müller, R., Stierhof, Y.-D., Gorb, S. and Schwarz, U. (2002). Chemical composition of the attachment pad secretion of the locust *Locusta migratoria*. *Insect Biochem. Mol. Biol.* **32**, 1605-1613.
- Walker, G., Yule, A. B. and Ratcliffe, J. (1985). The adhesive organ of the blowfly, *Calliphora vomitoria*: a functional approach (Diptera: Calliphoridae). *J. Zool. Lond.* **205**, 297-307.
- Way, M. J. and Murdie, G. (1965). An example of varietal resistance of Brussel sprouts. *Ann. Appl. Biol.* **56**, 326-328.
- Wu, W., Giese, R. F. and van Oss, C. J. (1995). Evaluation of the Lifshitz-van der Waals / acid-base approach to determine surface tension components. *Langmuir* **11**, 379-382.